Supplementary Information (SI) for Soft Matter.

Nature of barriers determine first passage times in heterogeneous media

Moumita Dasgupta,[1,*] Sougata Guha,[2,3,†] Leon Armbruster,[1] Dibyendu Das,[2,‡] and Mithun K. Mitra[2,§]

[1] *Department of Physics, Augsburg University, MN 55454, USA*
[2] *Department of Physics, IIT Bombay, Mumbai 400076, India*
[3] *INFN Napoli, Complesso Universitario di Monte S. Angelo, 80126 Napoli, Italy*

Supplementary Information

1. EXPERIMENT

A robotic bug (HEXBUG micro ant, $5cm \times 1.3cm$) (Fig. 3a in main text) powered by battery is used as a self propelled random walker. We characterized the motion of our random walker (RW) in different setups. First we consider a relatively large circular confinement of diameter $117cm$ (See Fig.∼3b in main text). MSD (Fig. 1c in main text) are calculated for approximately 25 trajectories with the RW moving outward from the center of the confinement to the boundary. The MSD of the bug has a superdiffusive behavior for shorter timescale with t∼1.8 which becomes subdiffusive over longer timescales with slopes between 0.5 and 1. To construct regions with a lower diffusion coefficient, we used wooden pegs of diameter $1cm$ arranged randomly at a packing fraction of 6% to constitute a crowded barrier region. A sample trajectory and MSDs are shown in Fig.(3e,f) in main text. The MSD varies with a lower slope t∼1.5 over a longer time compared to the empty case. The transport in this case is slowed down as compared to the free case due to repeated collision with the pegs, with the mean time to reach the boundary being $8.63 \pm 0.49sec$, as compared to a mean time of $3.95 \pm 0.39sec$ in the absence of barriers (Fig.3g in main text). The 6% packing fraction for the crowded region was determined experimentally based on the ease of turning of the robotic bug. Higher packing density resulted in the bug getting stuck between these crowders. We use this same density of pegs to construct rectangular barrier regions of dimensions $76cm \times 27cm$ (Fig. S1). For these rectangular barriers, the MFPT is about 2.5 times larger than for equivalent empty regions (Fig.3h in main text)

In our main experiments we had a rectangular length of dimension $180cm \times 76cm$ covered by an alternate barrier and empty regions. Two types of barrier regions are studied : entropic and energetic. For the entropic barriers, the pegs at 6% density filled a region of width $a = 20$ cm. Energetic barriers were made using styrofoams with 5 randomly-cut tunnels of size $3cm$. This tunnel size (slight larger than the HEXBUG) allows the RW to pass through in a near instantaneous manner (Suppl Fig. S2(a)). For experimental barrier widths $a = 20cm$, the passage times were $\lesssim 1s$. Further, we also quantified the number of attempts before the RW successfully enters a tunnel, which is indicative of hopping probability accross the energetic barrier (Suppl Fig. S2(b)). Note that statistical fluctuations are quite high due to the fact that first passage time distributions in confined spaces are typically exponential tailed. As is expected for an exponential distribution, the average is comparable to the standard deviation. Therefore to obtain a reliable estimate of MFPT, an optimum number of trials had to be chosen. We observed that beyond 60-65 trials, the MFPTs were converging to a steady value. Hence we used 100 trials for each setup. For energetic barriers, the slight increase in MFPT beyond $a/b > 2$ (Fig. 3d in main text), is an artefact of the finite size of our experimental setup. Around this width of the empty region ($b < 9$ cm), the dimensions of the RW become comparable to the width of the empty regions, and although the RW can still move, we do observe some significant restrictions in its turning behavior. The RW has a propensity to move preferentially only along the length of these narrow empty regions, without being able to turn randomly along the width - thereby increasing the overall MPFT. Since this behavior is not observed at any of the higher widths, this limitation of the system size is the cause for the higher MFPT values for $a/b > 2$.

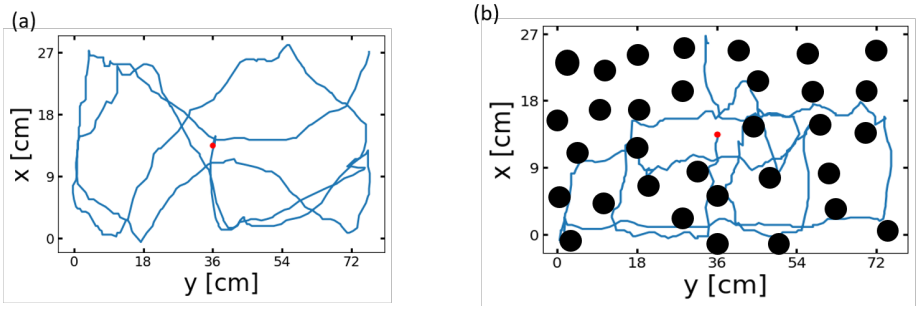

Fig. S1. (a) Sample trajectory of RW in empty region of dimensions $76 \times 27cm$. (b) Sample trajectory through obstacles of diameter 1 cm in a region of width 76×27 cm.

.

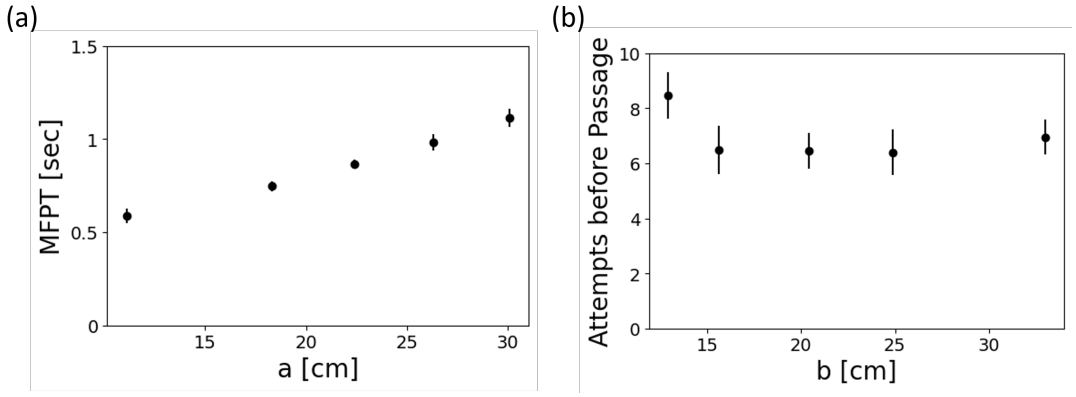

Fig. S2. (a) Mean First Passage Time (MFPT) to traverse the barrier (tunnel) regions for the case of energetic barrier. The times increase roughly linearly with the width of the barrier region, indicating ballistic transport through the tunnels, as expected. (b) The number of times the RW collides with the barrier interface before it successfully enters the barrier (tunnel) region for the case of energetic barriers. This is a intrinsic property of the barrier, and is experimentally seems to be independent of the width of the barrier regions, as expected.

2. EXPLICIT ANALYTIC RESULTS

2.1 ABSORBING BOUNDARY AT $r = r_0$

In the main manuscript we have derived MFPT for the case when absorbing boundary is located at $r = R$ and reflecting boundary at $r = r_0$. We now derive the opposite scenario where absorbing boundary is at $r = r_0$ and reflecting boundary is at $r = R$. Therefore, the boundary conditions in this case is given by,

$$\left.\frac{\partial\langle T_{2n+1}\rangle}{\partial r}\right|_R = 0, \qquad \text{and} \qquad \langle T_1\rangle|_{r_0} = 0 \tag{1}$$

From the above Eq. it is easy to obtain,

$$A_{n+1} = -\frac{R^d}{d} \tag{2}$$

$$\text{and} \quad B_1 = \begin{cases} -\frac{r_0^2}{2d} - \frac{A_1 r_0^{2-d}}{2-d}, & \text{for } d \neq 2 \\ -\frac{r_0^2}{2d} - A_1 \ \ln r_0, & \text{for } d = 2 \end{cases} \tag{3}$$

The matching conditions at barrier interfaces (Eqs. 6-9 and Eqs. 18-19 of the main text for entropic barriers and energetic barriers respectively) are independent of the choice of boundary conditions and hence the recursion relations given by Eqs. 12, 13, 14 and Eqs. 20, 21, 22 are still valid in this scenario.

Therefore, in this case , the MFPT of a diffusing particle starting from the reflecting boundary can be written as,

$$\tau = \langle T_{2n+}1\rangle|_R = \begin{cases} -\frac{1}{D_1}\left[\frac{R^2}{2d} + \frac{A_{n+1}R^{2-d}}{2-d} + B_{n+1}\right], \text{ for } d \neq 2 \\ -\frac{1}{D_1}\left[\frac{R^2}{2d} + A_{n+1}\ln R + B_{n+1}\right], \text{ for } d = 2 \end{cases} \tag{4}$$

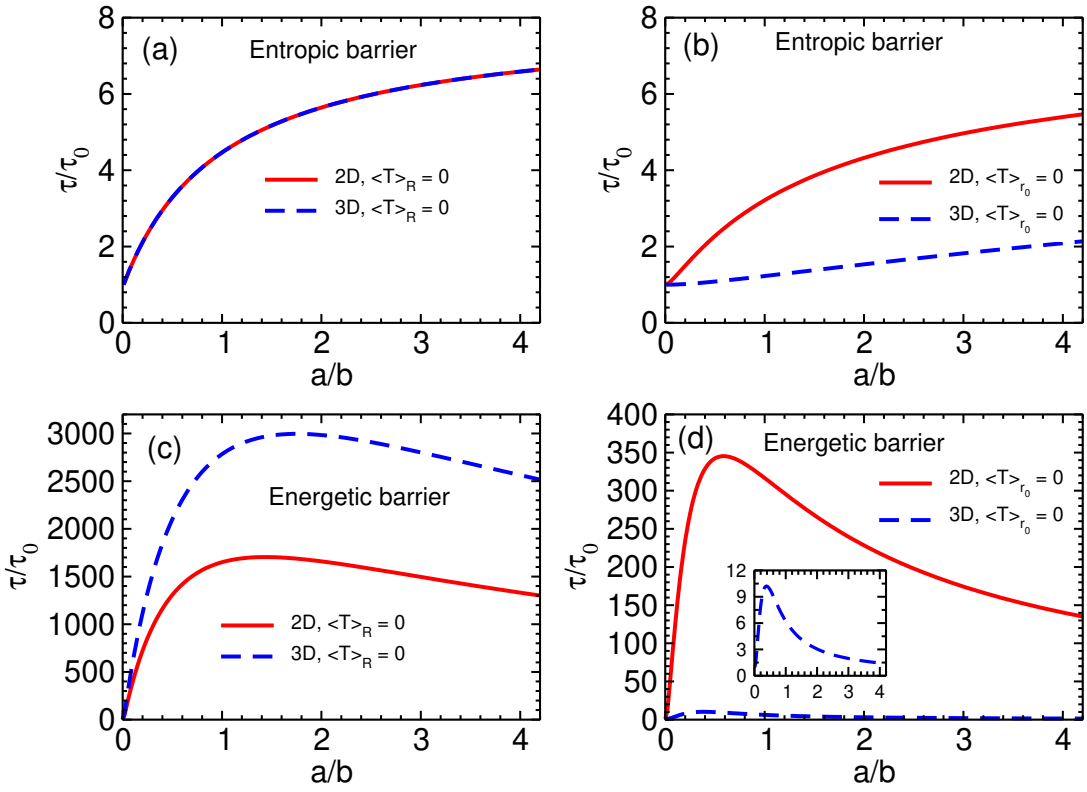

Fig. S3. Comparison of MFPT in 2D and 3D for two opposite set up. Panels (a) and (b) compares the results for entropic barriers when the absorbing boundary is at $r = R$ and $r = r_0$ respectively for $D_1/D_2 = 8$. Panels (c) and (d) shows the results for $(D_1/dv_q) = 50000$ when the absorbing boundary is at $r = R$ and $r = r_0$ respectively. A zoomed in version of the MFPT curve in 3D for absorbing boundary at $r = r_0$ is shown in panel (d) inset. The other chosen parameters are $a = 20$, $R = 2001$ and $r_0 = 1$.

where for entropic barriers,

$$B_{n+1} = \begin{cases} B_1 + \sum_{i=1}^{n} \frac{(s-1)}{2d} \left[r_{2i}^2 - r_{2i-1}^2\right] \\ + \sum_{i=1}^{n} \frac{(s-1)}{(2-d)} A_1 \left[r_{2i}^{2-d} - r_{2i-1}^{2-d}\right] & \text{for } d \neq 2 \\ B_1 + \sum_{i=1}^{n} \frac{(s-1)}{2d} \left[r_{2i}^2 - r_{2i-1}^2\right] \\ + \sum_{i=1}^{n} (s-1) A_1 \ \ln\left(\frac{r_{2i}}{r_{2i-1}}\right) & \text{for } d = 2 \end{cases}$$

and for energetic barriers,

$$B_{n+1} = \begin{cases} B_1 - \sum_{i=1}^{n} \frac{1}{2d} \left[r_{2i}^2 - r_{2i-1}^2\right] \\ - \sum_{i=1}^{n} A_i r_{2i-1}^{1-d} \left[\frac{a_i}{(2-d)} - \frac{D_1}{v_q}\right] \\ + \sum_{i=1}^{n} \frac{a_i r_{2i}}{d(2-d)} + \sum_{i=1}^{n} \frac{D_1 r_{2i-1}}{d v_q}, & \text{for } d \neq 2 \\ B_{n+1} - \sum_{i=1}^{n} \frac{1}{2d} \left[r_{2i}^2 - r_{2i-1}^2\right] \\ - \sum_{i=1}^{n} A_i r_{2i-1}^{1-d} \left[\frac{\ln r_{2i}}{r_{2i}^{1-d}} - \frac{\ln r_{2i-1}}{r_{2i-1}^{1-d}} - \frac{D_1}{v_q}\right] \\ + \sum_{i=1}^{n} \frac{a_i \ln r_{2i}}{d r_{2i}^{1-d}} + \sum_{i=1}^{n} \frac{D_1 r_{2i-1}}{d v_q}, & \text{for } d = 2 \end{cases}$$

2.2 ANALYTICAL CALCULATIONS FOR ONE-DIMENSION

While we present the general analytical formalism in d-dimensions in the main manuscript, for simplicity, we also explicitly solve the 1D case here.

2.2.1 ENTROPIC BARRIERS

Let us consider n barriers each of width a are distributed in region $x = 0$ and $x = L$.
The mean gap between two consecutive barriers is given by

$$b = \frac{L - na}{n + 1} \tag{5}$$

The boundary points of i^{th} barrier are denoted by x_{2i-1} and x_{2i} which can be expressed as

$$\begin{aligned} x_{2i-1} &= b + (i-1)(a+b) \qquad i \in (1, n) \\ x_{2i} &= i(a+b) \qquad\qquad\quad i \in (1, n) \end{aligned} \tag{6}$$

The MFPT in two regions obey

$$D_1 \frac{\partial^2 \langle T_{2i-1} \rangle}{\partial x^2} = -1 \qquad i \in (1, n+1) \tag{7}$$

$$D_2 \frac{\partial^2 \langle T_{2i} \rangle}{\partial x^2} = -1 \qquad i \in (1, n) \tag{8}$$

which has solutions

$$\langle T_{2i-1}(x) \rangle = -\frac{1}{D_1}\left[\frac{x^2}{2} + A_i x + B_i\right] \qquad i \in (1, n+1) \tag{9}$$

$$\langle T_{2i}(x) \rangle = -\frac{1}{D_2}\left[\frac{x^2}{2} + C_i x + E_i\right] \qquad i \in (1, n) \tag{10}$$

where A_i, B_i, C_i, E_i are the integrating constants.
The boundary conditions of the lattice boundaries are given as,

$$\partial_x < T_1 >_{x=0} = 0 \qquad \rightarrow \textit{reflecting boundary} \tag{11}$$

$$< T_{2n+1} >_{x=L} = 0 \qquad \rightarrow \textit{absorbing boundary} \tag{12}$$

The continuity MFPT at x_{2i-1} and x_{2i} gives,

$$\langle T_{2i-1} \rangle_{x_{2i-1}} = \langle T_{2i} \rangle_{x_{2i-1}} \qquad i \in (1, n) \tag{13}$$

$$\langle T_{2i} \rangle_{x_{2i}} = \langle T_{2i+1} \rangle_{x_{2i}} \qquad i \in (1, n) \tag{14}$$

Now the hopping dynamics that governs the motion can be written as,

$$\langle T_{2i-1} \rangle_{x_{2i-1}} = \frac{1}{p+q} + \frac{p}{p+q}\langle T_{2i-1} \rangle_{-\delta + x_{2i-1}} + \frac{q}{p+q}\langle T_{2i} \rangle_{\delta + x_{2i-1}} \tag{15}$$

$$\langle T_{2i+1} \rangle_{x_{2i}} = \frac{1}{p+q} + \frac{p}{p+q}\langle T_{2i+1} \rangle_{\delta + x_{2i}} + \frac{q}{p+q}\langle T_{2i} \rangle_{-\delta + x_{2i}} \tag{16}$$

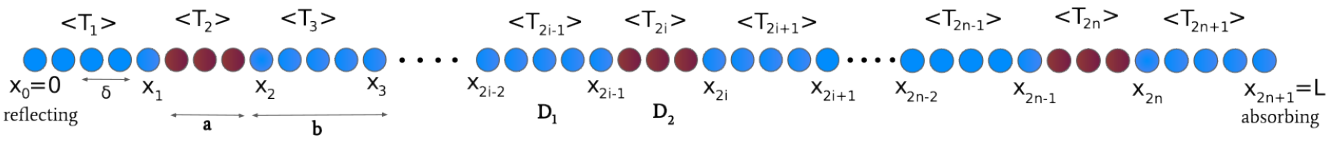

Fig. S4. Schematic of the system with n entropic barriers. The gap regions are denoted by blue and barriers are denoted by red. The boundary points of the i^{th} barrier are denoted by x_{2i-1} and x_{2i}. $\langle T_i \rangle$ denotes the mean average time for the particle to reach $x = L$ starting from the i^{th} region.

Now from Eq.15 we can write,

$$\begin{aligned}(p+q)\langle T_{2i-1}\rangle_{x_{2i-1}} &= 1+p\langle T_{2i-1}\rangle_{-\delta+x_{2i-1}}+q\langle T_{2i}\rangle_{\delta+x_{2i-1}}\\ \Rightarrow p\left[\langle T_{2i-1}\rangle_{x_{2i-1}}-\langle T_{2i-1}\rangle_{-\delta+x_{2i-1}}\right] &= 1+q\left[\langle T_{2i}\rangle_{\delta+x_{2i-1}}-\langle T_{2i-1}\rangle_{x_{2i-1}}\right]\end{aligned}$$

Using Eq.13 one can rewrite the above equation as,

$$\begin{aligned}p\left[\langle T_{2i-1}\rangle_{x_{2i-1}}-\langle T_{2i-1}\rangle_{-\delta+x_{2i-1}}\right] &= 1+q\left[\langle T_{2i}\rangle_{\delta+x_{2i-1}}-\langle T_{2i}\rangle_{x_{2i-1}}\right]\\ p\delta\left[\langle T_{2i-1}\rangle_{x_{2i-1}}-\langle T_{2i-1}\rangle_{-\delta+x_{2i-1}}\right] &= \delta+q\delta\left[\langle T_{2i}\rangle_{\delta+x_{2i-1}}-\langle T_{2i}\rangle_{x_{2i-1}}\right]\end{aligned}$$

Now taking $\delta\to 0$ we get,

$$\begin{aligned}p\delta^2\partial_x\langle T_{2i-1}\rangle_{x_{2i-1}} &= q\delta^2\partial_x\langle T_{2i}\rangle_{x_{2i-1}}\\ \Rightarrow D_1\partial_x\langle T_{2i-1}\rangle_{x_{2i-1}} &= D_2\partial_x\langle T_{2i}\rangle_{x_{2i-1}}\end{aligned} \tag{17}$$

Similarly from Eq.14 and Eq.16 one can write,

$$D_2\partial_x\langle T_{2i}\rangle_{x_{2i}} = D_1\partial_x < T_{2i+1} >_{x_{2i}} \tag{18}$$

Eqs.11,12,17 and 18 constitutes the boundary conditions for Eqs.9 and 10. From Eq.11 we have,

$$A_1 = 0 \tag{19}$$

Now, using Eq.17 and Eq.18 respectively we have,

$$C_i = A_i \tag{20}$$

$$A_{i+1} = A_i \tag{21}$$

Combining the Eqs.19,21,20 we get,

$$A_i = C_i = 0 \qquad \forall i = \{1, n+1\} \tag{22}$$

Now from Eq.13 we have,

$$B_i = (s-1)\frac{x_{2i-1}^2}{2} + sE_i \tag{23}$$

where $s = D_1/D_2$.
Using Eq.14 we have,

$$B_{i+1} = (s-1)\frac{x_{2i}^2}{2} + sE_i \tag{24}$$

Combining Eqs.23 and 24 we get,

$$B_{i+1} = B_i + \frac{(s-1)}{2}\left[x_{2i}^2 - x_{2i-1}^2\right] \tag{25}$$

Now from Eq.12 we have,

$$B_{n+1} = -\frac{x_{2n+1}^2}{2} = -\frac{L^2}{2} \tag{26}$$

Hence using Eq.25 we can write,

$$B_1 = B_{n+1} - \frac{(s-1)}{2}\sum_{i=1}^{n}\left(x_{2i}^2 - x_{2i-1}^2\right) \tag{27}$$

Therefore the MFPT of the particle to reach $x = L$ starting from $x = 0$ in presence of n barriers of width a is given by,

$$\begin{aligned}\tau &= \langle T_1\rangle_{x=0} = -\frac{B_1}{D_1}\\ &= \frac{1}{D_1}\left[\frac{L^2}{2} + \frac{(s-1)}{2}\sum_{i=1}^{n}\left(x_{2i}^2 - x_{2i-1}^2\right)\right]\end{aligned} \tag{28}$$

The summation in the above equation can be computed very easily.

$$\begin{aligned}\sum_{i=1}^{n}\left(x_{2i}^2-x_{2i-1}^2\right) &= \sum_{i=1}^{n}\left[i^2(a+b)^2-\{b+(i-1)(a+b)\}^2\right]\\ &= \sum_{i=1}^{n}\left[i^2(a+b)^2-\{i(a+b)-a\}^2\right]\\ &= \sum_{i=1}^{n}\left[2ia(a+b)-a^2\right]\\ &= n(n+1)a(a+b)-na^2=naL \end{aligned} \tag{29}$$

If τ_0 denotes the MFPT of the particle in absence of barriers then we have

$$\tau_0=\frac{L^2}{2D_1} \tag{30}$$

Therefore the scaled MFPT in presence of barriers is given by,

$$\begin{aligned}\frac{\tau}{\tau_0} &= \frac{2}{L^2}\left[\frac{L^2}{2}+\frac{(s-1)}{2}\sum_{i=1}^{n}\left(x_{2i}^2-x_{2i-1}^2\right)\right]\\ &= 1+\frac{(s-1)}{L^2}\cdot naL\\ &= 1+(s-1)\cdot\frac{na}{L}\\ &= 1+(s-1)\left(\frac{L-b}{a+b}\right)\frac{a}{L}\\ &= 1+(s-1)\frac{L\left(1-\frac{b}{L}\right)}{b\left(1+\frac{a}{b}\right)}\cdot\frac{a}{L}\\ &= 1+\frac{(s-1)\left(\frac{a}{b}-\frac{a}{L}\right)}{1+\frac{a}{b}}\end{aligned} \tag{31}$$

2.2.2 ENERGETIC BARRIERS

In the same spirit we shall now solve first passage time in case of energetic barriers. The hopping dynamics that determines the motion can be written as,

$$\begin{aligned}\langle T_{2i-1}\rangle_{x_{2i-1}} &= \frac{1}{p+q}+\frac{p}{p+q}\langle T_{2i-1}\rangle_{-\delta+x_{2i-1}}+\frac{q}{p+q}\langle T_{2i+1}\rangle_{x_{2i}}\\ \therefore p\left(\langle T_{2i-1}\rangle_{x_{2i-1}}-\langle T_{2i-1}\rangle_{-\delta+x_{2i-1}}\right) &= 1+q\langle T_{2i+1}\rangle_{x_{2i}}-q\langle T_{2i-1}\rangle_{x_{2i-1}}\\ \langle T_{2i-1}\rangle_{x_{2i-1}} &= \frac{1}{q}+\langle T_{2i+1}\rangle_{x_{2i}}-\frac{p\delta}{q}\partial_x\langle T_{2i-1}\rangle_{x_{2i-1}}\end{aligned} \tag{32}$$

Now we define $D_1=p\delta^2$ and $v_q=q\delta$ such that both D_1 and v_q are finite at $\delta\to 0$. Therefore we must have $p,q\to\infty$ and thus Eq.32 can be written as,

$$\langle T_{2i-1}\rangle_{x_{2i-1}}=\langle T_{2i+1}\rangle_{x_{2i}}-\frac{D_1}{v_q}\partial_x\langle T_{2i-1}\rangle_{x_{2i-1}} \tag{33}$$

Similarly it is easy to show that

$$\langle T_{2i-1}\rangle_{x_{2i-1}}=\langle T_{2i+1}\rangle_{x_{2i}}-\frac{D_1}{v_q}\partial_x\langle T_{2i+1}\rangle_{x_{2i}} \tag{34}$$

Hence from Eq.33 and Eq.34 we get,

$$\partial_x\langle T_{2i-1}\rangle_{x_{2i-1}}=\partial_x\langle T_{2i+1}\rangle_{x_{2i}} \tag{35}$$

For n energetic barriers, there will be n+1 fast regions where the particle diffuses. Therefore,

$$\langle T_{2i-1}\rangle = -\frac{1}{D_1}\left[\frac{x^2}{2} + A_i x + B_i\right] \tag{36}$$

where $i \in \{1, n+1\}$ denotes the region with boundaries x_{2i-2} and x_{2i-1} where the particle is in.
Now the lattice boundary conditions are same as Eq.11 and Eq.12,

$$\partial_x \langle T_1\rangle_{x=0} = 0 \tag{37}$$
$$\langle T_{2n+1}\rangle_{x=L} = 0 \tag{38}$$

Now Eq.37 gives

$$A_1 = 0$$

From Eq.35 we get,

$$A_{i+1} = A_i - a = A_1 - ia = -ia \tag{39}$$

Using Eq.38 we find B_{n+1} as,

$$B_{n+1} = -\frac{x_{2n+1}^2}{2} + nax_{2n+1} \tag{40}$$

where $x_{2n+1} = L = (n+1)(a+b) - a$.
Now from Eq.33 we can write,

$$B_i = B_{i+1} + \frac{1}{2}\left(x_{2i}^2 - x_{2i-1}^2\right) + \left(A_{i+1}x_{2i} - A_i x_{2i-1}\right) - \frac{D_1}{v_q}\left[x_{2i} + A_{i+1}\right] \tag{41}$$

Therefore

$$\begin{aligned} B_1 &= B_{n+1} + \sum_{i=1}^{n}\frac{1}{2}\left(x_{2i}^2 - x_{2i-1}^2\right) + \left(A_{i+1}x_{2i} - A_i x_{2i-1}\right) - \frac{D_1}{v_q}\left(x_{2i} + A_{i+1}\right) \\ \Rightarrow B_1 &= B_{n+1} - \frac{n(n-1)}{2}a^2 + \frac{n(n+1)D_1 a}{2v_q} - \frac{n(n+1)}{2}\left(\frac{D_1}{v_q} + a\right)(a+b) + \frac{1}{2}\sum_{i=1}^{n}\left(x_{2i}^2 - x_{2i-1}^2\right) \end{aligned} \tag{42}$$

Using Eq.6, Eq.29 and Eq.40, we can easily show from Eq.42 that

$$B_1 = -\frac{(n+1)^2 b^2 + n(n+1)\frac{D_1 b}{v_q}}{2} \tag{43}$$

The scaled first passage passage time then can be written as,

$$\frac{\tau}{\tau_0} = -\frac{2B_1}{L^2} = \frac{(n+1)^2 b^2 + n(n+1)\frac{D_1 b}{v_q}}{L^2}$$

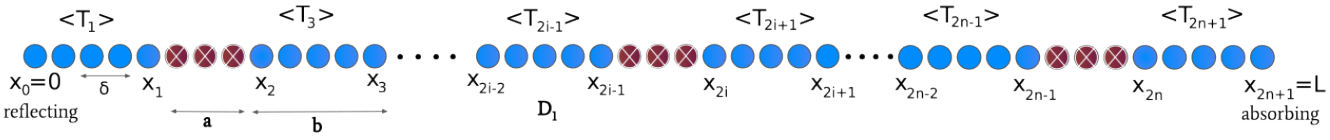

Fig. S5. Schematic of the system with n energetic barriers. The free regions are denoted by blue and barriers are denoted by red. The boundary points of the i^{th} barrier are denoted by x_{2i-1} and x_{2i}. $\langle T_{2i-1}\rangle$ denotes the mean time for the particle to reach $x = L$ starting from the i^{th} free region. Note that in this case $\langle T_{2i}\rangle$'s do not exist for all values of i.

Now using the relation $L = (n+1)(a+b) - a = n(a+b) + b$ one can write,

$$\begin{aligned}
\frac{\tau}{\tau_0} &= \frac{\frac{(L+a)^2}{(a+b)^2}b^2 + \left(\frac{L-b}{a+b}\right)\left(\frac{L+a}{a+b}\right)\frac{D_1 b}{v_q}}{L^2} \\
&= \frac{\frac{b^2(L+a)^2}{(a+b)^2} + \frac{(L^2+aL-bL-ab)}{(a+b)^2}\frac{D_1 b}{v_q}}{L^2} \\
&= \frac{\frac{b^2(L+a)^2}{L^2} + \frac{(L^2+aL-bL-ab)}{L^2}\frac{D_1 b}{v_q}}{(a+b)^2} \\
&= \frac{b^2\left(1+\frac{a}{L}\right)^2 + \left(1+\frac{a}{L}-\frac{b}{L}-\frac{ab}{L^2}\right)\frac{D_1 b}{v_q}}{(a+b)^2} \\
&= \frac{b^2\left(1+\frac{a}{L}\right)^2 + \left(\frac{L}{b}+\frac{a}{b}-1-\frac{a}{L}\right)\frac{D_1 b^2}{L v_q}}{(a+b)^2} \\
&= \frac{b^2\left(1+\frac{a}{L}\right)^2 + \left[\frac{a}{b}\left(\frac{L}{a}+1\right)-\frac{a}{L}\left(\frac{L}{a}+1\right)\right]\frac{D_1 b^2}{L v_q}}{b^2\left(1+\frac{a}{b}\right)^2} \\
&= \frac{\left(1+\frac{a}{L}\right)^2 + \left(\frac{a}{b}-\frac{a}{L}\right)\left(1+\frac{L}{a}\right)\frac{D}{L v_q}}{\left(1+\frac{a}{b}\right)^2}
\end{aligned} \tag{44}$$

3. EFFECTIVE DIFFUSIVITY

In this section, we investigate the long time diffusivity in the presence of barriers. Using kinetic simulations, we characterize the Mean Square Displacement (MSD) of the random walker as a function of elapsed time in an infinite lattice in the presence of barriers. Note that, while the first passage property is history-dependent, the MSD is not.

For entropic barriers, the MSD is shown for three different a/b ratios in Fig. **??**a. The RW initially explores the empty region in which it starts before it encounters the first barrier. This excursion is purely diffusive, with the bulk diffusion coefficient D_1, as is expected. At the timescale when it first encounters a barrier, the motion becomes subdiffusive as the barrier hinders the bulk diffusive behavior. Over long timescales ($t > 10^5$), the motion becomes diffusive again, however with an effective diffusion coefficient $D_{\rm eff}$ *i.e.* $\langle x^2(t)\rangle = 2D_{\rm eff}t$. The value of $D_{\rm eff}$ is lower than the bulk value D_1.

As a/b increases, and b decreases, with increasing n, the transition from early diffusive to a subdiffusive regime happens faster – for $a/b = 0.35, 1, 4$, the crossover times are $t \sim 10^3, 10^2, 5$ respectively. Moreover, with increasing a/b ratio the curves in Fig. **??**a at long times monotonically shift downwards. This in turn implies a monotonic decrease of $D_{\rm eff}$ as shown in Fig. **??**c. In 1D, the MFPT of a free region (in absence of barriers) is given by $\tau_0 = L^2/2D_1$. Analogously writing the MFPT of the heterogeneous medium as $\tau = L^2/2D_{\rm eff}$, it is easy to obtain the expression $D_{\rm eff}$ for the case $L \to \infty$. The Eq. 16 in the main text reads,

$$\begin{aligned}
\frac{\tau}{\tau_0} &= 1 + \frac{(s-1)(\frac{a}{b}-\frac{a}{L})}{1+\frac{a}{b}} \\
\Rightarrow \quad \frac{L^2/2D_{\rm eff}}{L^2/2D_1} &= 1 + \frac{(s-1)\frac{a}{b}}{1+\frac{a}{b}} \qquad [\ a/L \to 0 \text{ as } L \to \infty\ ] \\
\Rightarrow \quad D_{\rm eff} &= D_1\left(\frac{a+b}{as+b}\right)
\end{aligned} \tag{45}$$

The comparison of the simulation results with the effective diffusivity obtained from the theory is shown in Fig. **??**c. This monotonic behavior is consistent with the monotonic increase on the MFPT for entropic barriers in a finite domain.

Next we turn to a similar characterization for the energetic barriers. The MSD of the RW on an infinite lattice, as above, is again shown for three different a/b ratios in Fig. **??**b. Again, for all these case, there is an initial diffusive regime with a diffusivity D_1 of the empty regions. That crosses over to a subdiffusive regime when the RW starts to feel the effect of the barriers. As expected, this transition happens earlier for the highest number of barriers ($a/b = 4$),

and later with decreasing a/b ratios. In the long time limit, for all three a/b ratios shown, the motions are again diffusive, with $\langle x^2 \rangle = 2D_{\rm eff}t$. However, quite strikingly in Fig. **??**d, the MSD of the intermediate barrier number (with $a/b = 1$) lies below both the cases with lower and higher barrier numbers. As a result, as shown in Fig. **??**d, $D_{\rm eff}$ shows a non-monotonic behavior with increasing barrier number (or increasing a/b). Again, following the same method as before, one can obtain $D_{\rm eff}$ from Eq. 23 of main text,

$$\begin{aligned} \frac{\tau}{\tau_0} &= \frac{\left(1+\frac{a}{L}\right)^2 + \left(\frac{a}{b}-\frac{a}{L}\right)\left(\frac{1}{L}+\frac{1}{a}\right)\frac{D_1}{v_q}}{(1+\frac{a}{b})^2} \\ \Rightarrow \quad \frac{L^2/2D_1}{L^2/2D_{\rm eff}} &= \frac{1+\frac{D_1}{bv_q}}{\left(1+\frac{a}{b}\right)^2} \qquad [\ 1/L \to 0 \text{ as } L \to \infty\ ] \\ \Rightarrow \quad D_{\rm eff} &= D_1 \left(\frac{\left(1+\frac{a}{b}\right)^2}{1+\frac{D_1}{bv_q}} \right) \end{aligned} \tag{46}$$

The comparison between the analytical expression with the simulation results is shown in Fig. **??**d. Thus the signature of the non-monotonic dependence of the MFPT has its counterpart in the transport properties as well.

4. SUPERDIFFUSIVE MOTION

To generate a driven motion of the particle we follow the *Elephant-like memory diffusion* algorithm introduced by Schütz and Trimper in 2004 [1]. In this process the particle has complete memory of its previous steps. If at any time t the particle is at x_t then the evolution equation can be written as

$$x_{t+1} = x_t + \sigma_{t+1}$$

where σ_{t+1} is statistically chosen by the following method:

1. First a previous timestep $t' \in \{1, 2, ..., t\}$ is chosen randomly.
2. Then, $\sigma_{t+1} = \sigma_{t'}$ with probability w and $\sigma_{t+1} = -\sigma_{t'}$ with probability $1 - w$.

The particle starts at $x = 0$ at $t = 0$, and the first step of the particle is always towards positive direction in our simulation, i.e, $\sigma_1 = +1$.

The MSD in this type of non-Markovian process follows [1]:

$$\begin{aligned} \langle x_t^2 \rangle &\sim t \qquad \text{for} \quad w < 0.75 \\ &\sim t\ \ln t \quad \text{for} \quad w = 0.75 \\ &\sim t^{4w-2} \quad \text{for} \quad w > 0.75 \end{aligned}$$

For our simulations, we chose two values of $w = (0.875, 0.95)$ in the regime $w > 0.75$ to recover superdiffusive transport, as mentioned in the text.

* dasgupta@augsburg.edu; These authors contributed equally
† guha@na.infn.it; These authors contributed equally
‡ dibyendu@phy.iitb.ac.in
§ mithun@phy.iitb.ac.in

[1] Gunter M Schütz and Steffen Trimper. Elephants can always remember: Exact long-range memory effects in a non-markovian random walk. *Physical Review E*, 70(4):045101, 2004.